

Applied and
Computational
Mathematics
Division

NISTIR 89-4193

Center for Computing and Applied Mathematics

*A Numerical and Analytical Study of
Nonlinear Bifurcations Associated with the
Morphological Stability of Two-Dimensional
Single Crystals*

L.N. Brush, R.F. Sekerka and G.B. McFadden

October 1989

U.S. DEPARTMENT OF COMMERCE
National Institute of Standards and Technology
Gaithersburg, MD 20899

QC
100
.U56
89-4193
1989
C.2

NATIONAL INSTITUTE OF STANDARDS &
TECHNOLOGY
Research Information Center
Gaithersburg, MD 20899

NISTC
QC100
.456
NO. 89-4193
1989
C.2

A Numerical and Analytical Study of Nonlinear Bifurcations Associated with the Morphological Stability of Two-Dimensional Single Crystals

L. N. Brush

National Institute of Standards and Technology
Gaithersburg, MD 20899, USA

R. F. Sekerka

Carnegie Mellon University
Pittsburgh, PA 15213, USA

G.B. McFadden

National Institute of Standards and Technology
Gaithersburg, MD 20899, USA

Abstract

The nonlinear instability of a two-dimensional single crystal of pure material growing from an undercooled melt is studied both analytically and numerically. The quasi-steady state approximation is used for the thermal fields and the effects of different solid and liquid thermal conductivities and isotropic surface tension are included. A bifurcation analysis is performed by calculating the instantaneous value of the fundamental component of the local normal growth speed for an interface perturbed by a single Fourier shape component. The base state is time dependent, and two bifurcation criteria are studied, the relative stability criterion according to which the time derivative of the ratio of the perturbation amplitude to the radius of the underlying circle vanishes, and the absolute stability criterion according to which the time derivative of the perturbation amplitude vanishes. Numerically, the fundamental component of the interfacial growth speed is found by Fourier analysis of the solution to an integro-differential equation (obeyed at the interface) which gives the instantaneous value of the local normal growth speed. Analytically, a weakly nonlinear expansion technique is used to derive a solvability condition at each bifurcation. Our analytical and numerical results are in very close agreement, and therefore mutually corroborative. Landau coefficients are presented as a function of the various dimensionless parameters used in the model. Almost all of the bifurcations are subcritical.

1 Introduction

In this paper, we present a nonlinear bifurcation analysis for a single crystal of pure material growing from an undercooled melt in two dimensions. Our model couples the effects of isotropic surface tension with quasi-steady-state heat flow, according to which the thermal fields satisfy the Laplace equation throughout the bulk phases. We treat the case of isotropic surface tension but allow the conductivity in the crystal to differ from the conductivity of the melt. The nonlinear bifurcation analysis uses both numerical solutions to a fully nonlinear model of crystal growth as well as analytical (weakly nonlinear expansion) techniques.

To date, analytical work on nonlinear stability theory in solidification has focused primarily on exploring cellular interfaces that arise during directional solidification, and have small but finite amplitudes. Wollkind and Segal[1] were among the earliest authors to perform an analytical weakly nonlinear analysis for directional solidification in two dimensions. They investigated the weakly nonlinear interaction of a perturbation of fixed wavelength with itself. Wollkind and others[2, 3, 4] have continued this work, including three dimensional calculations. Wheeler[5], McFadden et al[6] and Ungar et al[7] have also performed analytical nonlinear calculations and have derived self-consistent evolution (Landau) equations for the perturbation amplitude as part of the stability analysis. Wheeler[5] and Dee and Mathur[8] have treated the case in which a band of wavelengths is considered, and McFadden et al[9] have included anisotropic surface tension in the weakly nonlinear analysis.

In this paper, we extend the analytical analysis used in directional solidification to the case of an initially circular single crystal growing into an undercooled melt. Furthermore,

we use a numerical method to compute the instantaneous growth velocity of the crystal-melt interface and compare these results with those obtained by an analytical method. The numerical (boundary integral) method is the same developed to calculate the evolving form of the crystal-melt interface during the free growth of a single crystal[10, 11].

In the following sections, we first present our model of crystal growth, including the integral equation that is used to determine numerically the local normal growth speed along the interface at a given time. We then give a brief description of the numerical method used to solve this integral equation and present our numerical results. The analytical nonlinear analysis follows, and a comparison between the analytical results and the numerical results is made.

2 The Model

We consider a two-dimensional single crystal of pure material, growing at the expense of a surrounding liquid phase due to the presence of an isothermal heat sink, at temperature T_∞ , located at a circular outer boundary of radius R'_∞ . In this model, lengths have been scaled by the nucleation radius $R^* = T_M\gamma/L(T_M - T_\infty)$ referred to the surface tension γ (assumed isotropic), where T_M is the bulk melting temperature, and times by $\tau = (R^*)^2/\alpha_L S$, where α_L is the thermal diffusivity of the liquid. Here $S = \rho_L c_L(T_M - T_\infty)/L$ is the dimensionless supercooling, in which ρ_L is the density of the liquid, c_L is its specific heat, and L is the latent heat per unit volume. The quantity S is assumed to be small, so that the quasi-steady state approximation (the Laplace equations in the bulk) is valid. Further details may be found

in previous references[10, 11]. We have assumed for the sake of simplicity that the densities of the two phases are equal ($\rho_L = \rho_S$), that the specific heats in the two phases are equal ($c_L = c_S$) and that there is no convection in the liquid. The governing equations in the bulk are:

$$\nabla^2 U_L = 0 \text{ (in the melt)} \quad (1)$$

and

$$\nabla^2 U_S = 0 \text{ (in the crystal),} \quad (2)$$

where $U_{S,L} = (T_{S,L} - T_\infty)/(T_M - T_\infty)$ is the dimensionless temperature in the crystal (S) or in the melt (L). At the far boundary, $U_L = 0$ and at the crystal-melt interface:

$$U_{S,L} = 1 - K, \quad \text{and} \quad (3)$$

$$V_N = [-\nabla U_L + \beta \nabla U_S] \cdot \hat{n}, \quad (4)$$

where K is the (dimensionless) local curvature, V_N is the local normal growth speed, $\beta = k_S/k_L$ is the ratio of the thermal conductivities, and \hat{n} is the normal vector to the interface pointing into the liquid phase.

3 Numerical Method

3.1 Integral Equation Method

Eqns. (1) through (4) may be reformulated into a single boundary integral equation. We

define the variable α as the quotient of the arclength s to the perimeter S_T of the interface; then, for a given point on the interface, α_o , the result is,

$$\begin{aligned} \left[\frac{1 + \beta}{2} \right] U_I(\alpha_o) &= S_T \int G(\alpha, \alpha_o) V_N(\alpha) d\alpha \\ &+ S_T [1 - \beta] \int U_I(\alpha) \nabla G(\alpha, \alpha_o) \cdot \hat{n}(\alpha) d\alpha, \end{aligned} \quad (5)$$

in which $G(\alpha, \alpha_o)$ is the Green's function (see [11] for details) for a circle of radius R_∞ , and $U_I = 1 - K$ is the interfacial temperature. The solution to the integral equation (5) will give $V_N(\alpha_o)$ (the local normal growth speed) at any instant of time. This equation is solved by numerical methods described previously [10, 11].

3.2 Numerical Results

We assume an interface shape given by $r = R + A \cos(k\theta)$ and choose values of the radius R , the amplitude A , the ratio of the solid to liquid thermal conductivities β , and the dimensionless parameter R_∞ . We use the numerical method referenced in the previous section to solve the integral equation (5) for the local normal growth speed along the interface at a given time. Fourier analysis of the solution enables us to determine the fundamental Fourier component, $V_N(k, A)$, of the growth speed from the numerical solution. We investigate the manner in which $V_N(k, A)$ changes as a function of the amplitude A of the perturbation. As the amplitude of the shape perturbation increases, the solution of Eqn. (5) displays increasingly nonlinear behavior, affecting $V_N(k, A)$, and causing higher order harmonics, $V_N(nk, A)$, in the velocity Fourier spectrum to grow.

Examples of the nonlinear behavior of the fundamental component of the velocity $V_N(k, A)$ as a function of the increase of the amplitude of a perturbation having a four-fold symmetry, ($k = 4$), are shown in Figures (1) and (2). In these calculations $R < R_{cr}$, in which R_{cr} is the critical radius at which the fundamental component of the velocity vanishes. R_{cr} may be found by using linear perturbation theory and is a root of [12]

$$\left(\frac{1 - (1/R_{cr})}{\ln(R_{cr}/R_\infty)} \right) \left[1 - \frac{k}{M} \right] + \left(\frac{k(1 - k^2)}{R_{cr}} \right) \left[\frac{1}{M} + \beta \right] = 0, \quad (6)$$

$$\text{with } M = \left(1 - \left(\frac{R_{cr}}{R_\infty} \right)^{2k} \right) / \left(1 + \left(\frac{R_{cr}}{R_\infty} \right)^{2k} \right).$$

In Figs. (1) and (2), each curve represents a specific value of the crystal's mean radius R . In Figure (1), we have taken the thermal conductivities in both phases to be equal, while for Figure (2), $\beta = 2$. We define the critical amplitude A_{nl} to be the finite amplitude for which $V_N(k, A) = 0$, and in Fig. (3), A_{nl} is plotted as a function of R under conditions given in Fig. (1). As the departure of the average crystal size below the critical radius increases, the critical amplitude becomes larger.

Numerical analysis of the Fourier components of the growth speed shows that the fundamental Fourier component of the interface velocity obeys, to a good approximation, the equation

$$V_N(k, A) = C_1 A \left(1 - \left(\frac{A}{A_{nl}} \right)^2 \right), \quad (7)$$

in which C_1 may be calculated from linear stability theory and changes from negative to positive as the radius changes from below to above the critical radius, and A_{nl} denotes the numerical value of the critical amplitude for a given radius R . Furthermore, as the amplitude

A increases, higher order harmonics $V_N(nk, A)$ will appear in the Fourier spectrum of the velocity. As the higher order harmonics begin to grow large, the second harmonic of the velocity field is a linear function of A^2 , while the third harmonic of the velocity is a linear function of A^3 and so on. Thus, $V_N(nk, A) = C_n A^n$ for A sufficiently small. We show an example of these results in Table (1). In the next section, we use an analytical weakly nonlinear analysis to reproduce the numerically predicted nonlinear bifurcation, and to gain further insight into the nature of the bifurcation.

4 Weakly Nonlinear Analysis

The analytical nonlinear stability analysis presented in this work differs from previous nonlinear analyses for the following reasons. First, the geometry of the unperturbed single crystal (the shape about which the nonlinear expansion is performed) is circular, not planar. Second, the base state is neither quiescent, steady-state nor time periodic. Our analysis therefore results in instantaneous stability conditions because during free growth, the coupling of all growing Fourier components acts to change the crystal shape in the next instant in time.

In order to investigate finite amplitude effects, we assume that a circular crystal is perturbed by a single Fourier component of integer wavenumber k , so that $r(\theta) = R + A \cos(k\theta)$. We fix the wavenumber of the perturbation and investigate the weakly nonlinear interaction of a perturbation of given wavelength with itself. Our strategy is to fix the radius, R , and find the amplitude A_{nl} for which the fundamental component of the interfacial velocity is

zero. We assume that the mean radius of the crystal, the shape perturbation amplitude, the liquid and solid temperatures and the velocity of the interface may be expanded in powers of a small parameter ϵ ,

$$R(\epsilon) = \sum_{n=0}^{\infty} \epsilon^n R^{(n)} \quad (8)$$

$$r(\theta, \epsilon) = \sum_{n=0}^{\infty} \epsilon^n R^{(n)} + \left(\sum_{n=1}^{\infty} \epsilon^n \rho_{n1} \right) \cos(k\theta) = \sum_{n=0}^{\infty} \epsilon^n Z^{(n)}(\theta), \quad (9)$$

$$U(r, \theta, \epsilon) = U^{(0)}(r) + \epsilon U^{(1)}(r, \theta) + \epsilon^2 U^{(2)}(r, \theta) + \epsilon^3 U^{(3)}(r, \theta) + \dots, \text{ and} \quad (10)$$

$$V_N(\theta, \epsilon) = V_N^{(0)} + \epsilon V_N^{(1)}(\theta) + \epsilon^2 V_N^{(2)}(\theta) + \epsilon^3 V_N^{(3)}(\theta) + \dots \quad (11)$$

in which $Z^{(n)}(\theta) = R^{(n)} + \rho_{n1} \cos(k\theta)$, and $\rho_{01} = 0$. The velocity V_N is composed of Fourier components at each order of ϵ . We substitute Eqns. (8) to (11) into Eqns. (1) to (4), expand all boundary conditions in a series about the unperturbed circular radius, $R^{(0)}$, for which $\epsilon = 0$, and obtain a system of equations at each order of the expansion parameter ϵ . For the zero order problem we have

$$\frac{\partial^2 U_S^{(0)}}{\partial r^2} + \left(\frac{1}{r}\right) \frac{\partial U_S^{(0)}}{\partial r} = 0, \text{ for } r < R^{(0)}, \text{ with } U_S^{(0)}(r=0) < \infty, \text{ and} \quad (12)$$

$$\frac{\partial^2 U_L^{(0)}}{\partial r^2} + \left(\frac{1}{r}\right) \frac{\partial U_L^{(0)}}{\partial r} = 0, \text{ for } R^{(0)} < r < R_{\infty}, \text{ with } U_L^{(0)}(r=R_{\infty}) = 0, \quad (13)$$

in the bulk phases, and

$$U_S^{(0)} = 1 - \frac{1}{R^{(0)}}, \quad (14)$$

$$U_L^{(0)} = 1 - \frac{1}{R^{(0)}} \quad \text{and}$$

$$V_N^{(0)} = (-DU_L^{(0)} + \beta DU_S^{(0)}),$$

at $r = R^{(0)}$. D denotes the derivative of a function with respect to r . For all other orders, ϵ^n , the equations in the bulk are

$$\nabla^2 U_S^{(n)} = 0, \text{ for } r < R^{(0)}, \text{ with } U_S^{(n)}(r = 0) < \infty, \text{ and} \quad (15)$$

$$\nabla^2 U_L^{(n)} = 0, \text{ for } R^{(0)} < r < R_\infty, \text{ with } U_L^{(n)}(r = R_\infty) = 0, \quad (16)$$

and the boundary conditions are

$$U_S^{(n)} + Z^{(n)} (DU_S^{(0)}) - \left(\frac{Z^{(n)} + (Z^{(n)})_{\theta\theta}}{(R^{(0)})^2} \right) = C_n, \quad (17)$$

$$U_L^{(n)} + Z^{(n)} (DU_L^{(0)}) - \left(\frac{Z^{(n)} + (Z^{(n)})_{\theta\theta}}{(R^{(0)})^2} \right) = D_n, \text{ and}$$

$$V_N^{(n)} - D (-U_L^{(n)} + \beta U_S^{(n)}) + Z^{(n)} (D^2(U_L^{(0)} - \beta U_S^{(0)})) = E_n,$$

in which all functions are evaluated at the unperturbed radius $R^{(0)}$. The subscripts θ refer to derivatives with respect to the polar angle θ . At any order, say $O(\epsilon^n)$, the inhomogeneous terms in Eqns. (17), C_n , D_n and E_n , depend only on the solutions at $O(\epsilon^{n-1})$ or lower. These inhomogeneous terms are listed in the Appendix. The set of equations at each order in ϵ is linear, and our solution procedure is to solve this set of equations up to order ϵ^3 .

4.1 Zero Order (Unperturbed) Solution

The zero order (ϵ^0) problem gives the unperturbed circular solution. The growth velocity is

$$V_N^{(0)} = \left(1 - \frac{1}{R^{(0)}} \right) / \left(R^{(0)} \ln \left(\frac{R_\infty}{R^{(0)}} \right) \right), \quad (18)$$

and the solutions for the unperturbed thermal fields are

$$U_S^{(0)}(r) = 1 - \frac{1}{R^{(0)}} \quad \text{and} \quad (19)$$

$$U_L^{(0)}(r) = B_0 \ln\left(\frac{r}{R_\infty}\right),$$

in which

$$B_0 = \left(1 - \frac{1}{R^{(0)}}\right) / \left(\ln\left(\frac{R^{(0)}}{R_\infty}\right)\right). \quad (20)$$

4.2 First Order Solution

In order to find a solution to the set of differential equations at first order in ϵ , we assume solutions of the form

$$U_{S,L}^{(1)}(r, \theta) = U_{S,L}^{(10)}(r) + U_{S,L}^{(11)}(r) \cos(k\theta), \quad (21)$$

$$Z^{(1)}(\theta) = R^{(1)} + \rho_{11} \cos(k\theta) \quad \text{and}$$

$$V_N^{(1)} = V_N^{(10)} + V_N^{(11)} \cos(k\theta).$$

Analysis of the boundary conditions (Eqns. (17)) shows that the differential equations and the boundary conditions are satisfied identically if we set $R^{(1)} = 0$, in which case $U_{S,L}^{(10)}$ and $V_N^{(10)}$ also vanish. In order to find the critical amplitude, we must require the first order contribution to the fundamental component of the local normal growth speed $V_N^{(11)}$ to vanish. This condition reproduces the marginal stability results of linear theory. Setting $R^{(1)}$, $U_S^{(10)}$, $U_L^{(10)}$, $V_N^{(10)}$ and $V_N^{(11)}$ to zero, Eqns. (21) are substituted into Eqns. (15) and (16), from which the solutions

$$U_S^{(11)}(r) = A_S^{(11)} r^k \quad \text{and} \quad (22)$$

$$U_L^{(11)}(r) = \frac{B_L^{(11)}}{R_\infty^k} \left(\frac{R_\infty^k}{r^k} - \frac{r^k}{R_\infty^k} \right)$$

are determined. The unknown solution constants, $A_S^{(11)}$, $B_L^{(11)}$ and ρ_{11} , satisfy the matrix equation,

$$P_{11} \vec{X}_{11} = \vec{0}, \quad (23)$$

in which $\vec{X}_{11} = (A_S^{(11)}, B_L^{(11)}, \rho_{11})^T$, and P_{11} is the matrix

$$\begin{pmatrix} (R^{(0)})^k & 0 & -((1-k^2)/(R^{(0)})^2) \\ 0 & 1/(R^k) (1 - (R^{(0)}/R_\infty)^{2k}) & (B_0/R^{(0)} - (1-k^2)/(R^{(0)})^2) \\ -\beta k (R^{(0)})^{k-1} & -k/(R^{k+1}) (1 + (R^{(0)}/R_\infty)^{2k}) & -(B_0/(R^{(0)})^2) \end{pmatrix}. \quad (24)$$

In order to obtain non-trivial solutions to the homogeneous system, the determinant of P_{11} must vanish, thereby determining the marginal stability condition and defining the corresponding marginal stability radius $R^{(0)} = R_{cr}$. The marginal stability condition has already been given in Eqn. (6). The solutions to the first order problem may be written in terms of a single undetermined coefficient ρ_{11} in the form:

$$U_S^{(1)}(r, \theta) = \left(\frac{(1-k^2)}{R_{cr}^{2+k}} \right) r^k \rho_{11} \cos(k\theta) \quad (25)$$

in the crystal, and

$$\begin{aligned} U_L^{(1)}(r, \theta) = & - \left(\frac{B_0}{R_{cr}} - \frac{(1-k^2)}{(R_{cr})^2} \right) \left(\frac{R_{cr}^k}{R_\infty^k} \right) \left(1 - \left(\frac{R_{cr}}{R_\infty} \right)^{2k} \right)^{-1} \\ & \times \left(\frac{R_\infty^k}{r^k} - \frac{r^k}{R_\infty^k} \right) \rho_{11} \cos(k\theta) \end{aligned} \quad (26)$$

in the melt.

4.3 Second Order Solution

Expanding the right hand sides of the boundary conditions, Eqns. (17), gives

$$C_2 = C_{20} + C_{22} \cos(2k\theta), \quad (27)$$

$$D_2 = D_{20} + D_{22} \cos(2k\theta) \text{ and}$$

$$E_2 = E_{20} + E_{22} \cos(2k\theta)$$

in which C_{20} , C_{22} , D_{20} , D_{22} , E_{20} and E_{22} are given in the Appendix. Since the second order equations are linear, we may assume solutions of the form

$$U_{S,L}^{(2)}(r, \theta) = U_{S,L}^{(20)}(r) + U_{S,L}^{(22)}(r) \cos(2k\theta), \quad (28)$$

$$Z^{(2)} = R^{(2)}, \text{ and}$$

$$V_N^{(2)} = V_N^{(20)} + V_N^{(22)} \cos(2k\theta).$$

Equations (28) are substituted into Laplace's equation, and each Fourier component of the solution of the system of linear equations is solved independently. The solutions are

$$U_S^{(20)}(r) = A_S^{(20)}, \quad (29)$$

$$U_L^{(20)}(r) = B_L^{(20)} \ln \left(\frac{r}{R_\infty} \right)$$

and

$$U_S^{(22)}(r) = A_S^{(22)} r^{2k}, \quad (30)$$

$$U_L^{(22)}(r) = \frac{B_L^{(22)}}{R_\infty^{2k}} \left(\frac{R_\infty^{2k}}{r^{2k}} - \frac{r^{2k}}{R_\infty^{2k}} \right).$$

Eqns. (29) and (30) are then substituted into the interfacial conditions whereupon $A_S^{(20)}$, $B_L^{(20)}$ and $V_N^{(20)}$ are found from the solution of

$$A_S^{(20)} - \frac{R^{(2)}}{R_{cr}^2} = C_{20}, \quad (31)$$

$$B_L^{(20)} \ln \frac{R_{cr}}{R_\infty} + R^{(2)} \left(\frac{B_0}{R_{cr}} - \frac{1}{R_{cr}^2} \right) = D_{20}, \quad \text{and}$$

$$V_N^{(20)} + \frac{B_L^{(20)}}{R_{cr}} - R^{(2)} \left(\frac{B_0}{R_{cr}^2} \right) = E_{20}.$$

At this stage, we appear to have six unknowns, $A_S^{(20)}$, $B_L^{(20)}$, $V_N^{(20)}$, $R^{(2)}$, ρ_{11} and ϵ , but only three equations. A degree of freedom, however, has been caused by the introduction of the expansion parameter ϵ , and this allows for an arbitrary but convenient choice for ϵ . Thus, to second order in ϵ , only the quantities $\epsilon^2 R^{(2)} = R - R_{cr}$ and $\epsilon \rho_{11} = A$ have physical meaning. For example, if we choose $\epsilon = (R_{cr} - R)^{1/2}$ (or equivalently $R^{(2)} = -1$) in which $R < R_{cr}$ is the actual radius of the crystal (which would be an appropriate choice for a subcritical instability) the nonlinear analysis could then be continued to third order to calculate the value of the critical amplitude $A = A_{nl}$ as a function of $R = R_{nl}$ at the nonlinear bifurcation point. An alternative strategy is to choose $\epsilon = A$ (or equivalently $\rho_{11} = 1$) and then to calculate the value of $R - R_{cr} = R_{nl} - R_{cr}$ as a function of A_{nl} at the bifurcation point from the nonlinear analysis. The sign of $R_{nl} - R_{cr}$ indicates whether the bifurcation is “supercritical” or “subcritical”. For the moment we choose to retain flexibility and express the solutions at second order as functions of the two expansion parameters, $R^{(2)}$ and ρ_{11} .

With the aid of Eqns. (31), the solutions $U_S^{(20)}$ and $U_L^{(20)}$, and the velocity component $V_N^{(20)}$ may be written in the form

$$U_S^{(20)} = C_{20} + \frac{R^{(2)}}{R_{cr}^2}, \quad (32)$$

$$U_L^{(20)} = \left(D_{20} - R^{(2)} \left(\frac{B_0}{R_{cr}} - \frac{1}{R_{cr}^2} \right) \right) \frac{\ln(r/R_\infty)}{\ln(R_{cr}/R_\infty)} \quad \text{and}$$

$$V_N^{(20)} = E_{20} + R^{(2)} \frac{B_0}{R_{cr}^2} - \left(D_{20} - R^{(2)} \left(\frac{B_0}{R_{cr}} - \frac{1}{R_{cr}^2} \right) \right) (R_{cr} \ln(R_{cr}/R_\infty))^{-1}.$$

The solution constants $A_S^{(22)}$, $B_L^{(22)}$ and $V_N^{(22)}$ are determined by using the boundary conditions corresponding to the $\cos(2k\theta)$ problem and lead to the matrix equation

$$P_{22} \vec{X}_{22} = \vec{R}_{22} \quad (33)$$

in which $\vec{X}_{22} = (A_S^{(22)}, B_L^{(22)}, V_N^{(22)})^T$, $\vec{R}_{22} = (C_{22}, D_{22}, E_{22})^T$ and P_{22} is the matrix

$$\begin{pmatrix} (R^0)^{2k} & 0 & 0 \\ 0 & 1/(R^k)^2 (1 - (R^0/R_\infty)^{4k}) & 0 \\ -2\beta k (R^0)^{2k-1} & -2k/(R^{2k+1}) (1 + (R^0/R_\infty)^{4k}) & 1 \end{pmatrix}. \quad (34)$$

By solving Eqn. (33), we determine the solutions

$$U_S^{(22)}(r) = C_{22} \left(\frac{r}{R_{cr}} \right)^{2k} \quad (35)$$

$$U_L^{(22)}(r) = \frac{R_{cr}^{2k}}{R_\infty^{2k}} \left(\frac{R_\infty^{2k}}{r^{2k}} - \frac{r^{2k}}{R_\infty^{2k}} \right) \left(1 - \left(\frac{R_{cr}}{R_\infty} \right)^{4k} \right)^{-1} D_{22}, \quad \text{and}$$

$$V_N^{(22)} = E_{22} + \left(\frac{2k\beta}{R_{cr}} \right) C_{22} + \left(\frac{2k}{R_{cr} M_4} \right) D_{22}.$$

We emphasize that although the interface shape consists of only a single Fourier component (proportional to $\cos(k\theta)$), there exists a Fourier component of the velocity proportional to $\cos(2k\theta)$. We may not assume that this component of the velocity is zero, for then the analysis leads to an overdetermined system of equations. Therefore, the nonlinear analysis gives only an instantaneous condition for the disappearance of the fundamental Fourier component of the velocity. Since this second order solution does not determine a relationship between ρ_{11} and $R^{(2)}$ (or equivalently between A_{nl} and R_{nl}) we proceed to the third order problem.

4.4 Third Order Solution

We expand the right hand sides of the inhomogeneous third order boundary conditions (17) to find

$$C_3 = C_{31} \cos(k\theta) + C_{33} \cos(3k\theta), \quad (36)$$

$$D_3 = D_{31} \cos(k\theta) + D_{33} \cos(3k\theta),$$

$$E_3 = E_{31} \cos(k\theta) + E_{33} \cos(3k\theta),$$

From the Appendix we see that C_{31} , D_{31} and E_{31} are of the form

$$C_{31} = C_{313}\rho_{11}^3 + C_{311}\rho_{11} \quad (37)$$

$$D_{31} = D_{313}\rho_{11}^3 + D_{311}\rho_{11}$$

$$E_{31} = E_{313}\rho_{11}^3 + E_{311}\rho_{11}$$

(The remaining coefficients C_{33} , D_{33} and E_{33} are not needed for the analysis.) Consistent with Eqns. (36), we assume solutions at third order of the form

$$U_{S,L}^{(3)}(r, \theta) = U_{S,L}^{(31)}(r) \cos(k\theta) + U_{S,L}^{(33)}(r) \cos(3k\theta), \quad (38)$$

$$Z^{(3)}(\theta) = \rho_{31} \cos(k\theta), \quad \text{and}$$

$$V_N^{(3)} = V_N^{(31)} \cos(k\theta) + V_N^{(33)} \cos(3k\theta).$$

These are substituted into the Laplace equations and the resulting solutions are then applied to the third order boundary conditions to give

$$P_{11} \vec{X}_{31} = \vec{R}_{31}, \quad (39)$$

for the $\cos(k\theta)$ component, for which we seek the unknown vector $\vec{X}_{31} = (A_S^{(31)}, B_L^{(31)}, \rho_{31})^T$. In Eqn. (39), the right hand side $\vec{R}_{31} = (C_{31}, D_{31}, E_{31})^T$; furthermore $V_N^{(31)}$ has been set to zero because we are seeking the marginal stability condition. The determinant of P_{11} vanishes (because the radius has been set at R_{cr} in the first order problem); thus, in order for a solution \vec{X}_{31} to exist, the solvability condition

$$\left(\vec{R}_{31}, \vec{y} \right) = 0 \quad (40)$$

must be obeyed (in which the parentheses denote the inner product of \vec{R}_{31} and \vec{y}) for all vectors \vec{y} satisfying $P_{11}^A \vec{y} = 0$ where P_{11}^A is the adjoint of the matrix P_{11} . Evaluation of Eqn.

(40) leads to the solvability condition

$$C_{31} + \left(\frac{R_{cr}}{k\beta} \right) E_{31} + \left(\frac{1}{\beta M} \right) D_{31} = 0. \quad (41)$$

Substitution of Eqn. (37) for C_{31} , D_{31} and E_{31} into Eqn. (41) leads to the following system of equations relating $R^{(2)}$, ρ_{11} and ϵ :

$$\Omega \rho_{11}^3 - R^{(2)} \Upsilon \rho_{11} = 0, \quad (42)$$

$$A_{nl} = \epsilon \rho_{11}, \text{ and}$$

$$R_{nl} = R_{cr} + \epsilon^2 R^{(2)}.$$

The coefficients Υ and Ω are given in the Appendix. Eqns. (42) give,

$$R_{nl} - R_{cr} = A_{nl}^2 \frac{\Omega}{\Upsilon} \quad (43)$$

which is the central analytical result. In the following section we compare Eqn. (43) with our numerical results and characterize the nature of the bifurcation over a range of material parameters.

5 Analytical Results

5.1 Comparison with Numerical Results

To verify the accuracy of our calculations, we compare the values of the subcritical amplitude A_{nl} for given R_{nl} determined by the numerical solution of Eqn. (5) with the value found by using the weakly nonlinear stability analysis. In Fig. (4), we examine the case for which the ratio of the thermal conductivities is unity and $k = 4$. We plot $\ln(A_{nl})$ as a function of $1/2 \ln(R_{cr} - R_{nl})$ and observe that the numerical calculations (denoted by the open boxes)

lie directly on top of the straight line of unit slope representing the analytical calculation. Our numerical and analytical results are therefore, mutually corroborative. In Table (2), a further comparison between the values of the numerical and the analytical calculations is presented. In Tables (3) and (4), we list the values of $A_{nl}/(R_{cr} - R_{nl})^{1/2}$ corresponding to the point of subcritical instability as the value of the dimensionless parameter R_∞ increases for fixed β , and as the value of the ratio of the thermal conductivities β increases for fixed R_∞ . Table (3) indicates a very weak (essentially logarithmic) dependence on R_∞ as expected; Table (4) indicates that as β decreases, the bifurcation becomes more strongly subcritical.

5.2 Relative and Absolute Stability Criteria

We have computed the stability condition for which the fundamental component of the growth speed vanishes, sometimes called absolute stability[12]. (This is not to be confused with the Mullins and Sekerka usage of absolute stability[13].) Insofar as shape changes are concerned, however, this is not the most meaningful criterion; even though a perturbation may be growing, A/R may be decaying. A more meaningful criterion is that of relative stability, the point at which the time derivative of the ratio of the perturbation amplitude to the underlying crystal radius vanishes. To third order in ϵ this condition is given by,

$$\frac{d}{dt} \left(\frac{A}{R} \right) = \left(\frac{\epsilon V_N^{(11)} + \epsilon^3 V_N^{(31)}}{R^{(0)} + \epsilon^2 R^{(2)}} \right) - \left(\frac{(\epsilon \rho_{11} + \epsilon^3 \rho_{31})(V_N^{(0)} + \epsilon^2 V_N^{(20)})}{(R^{(0)} + \epsilon^2 R^{(2)})^2} \right) = 0. \quad (44)$$

Eqn. (44) requires that at the point of relative instability,

$$V_N^{(11)} = \frac{V_N^{(0)} \rho_{11}}{R^{(0)}}, \text{ and} \quad (45)$$

$$V_N^{(31)} = \frac{(V_N^{(20)} \rho_{11} + \rho_{31} V_N^{(0)})}{R^{(0)}} - \frac{R^{(2)} \rho_{11} V_N^{(0)}}{(R^{(0)})^2}.$$

The algebraic differences between the relative stability point and the absolute stability point are the following: at first order, the homogeneous boundary conditions may be written

$$P_{11}^* \vec{X}_{11} = \vec{0}, \quad (46)$$

where P_{11}^* is the matrix

$$P_{11}^* + \begin{pmatrix} 0 & 0 & 0 \\ 0 & 0 & 0 \\ 0 & 0 & -(B_0/(R^{(0)})^2) \end{pmatrix}. \quad (47)$$

The critical radius R_{cr}^* , denoting the onset of relative instability, is now given by the roots of[12]

$$\left(\frac{1 - (1/R_{cr}^*)}{\ln(R_{cr}^*/R_\infty)} \right) \left[2 - \frac{k}{M} \right] + \left(\frac{k(1 - k^2)}{R_{cr}^*} \right) \left[\frac{1}{M} + \beta \right] = 0. \quad (48)$$

At third order the boundary conditions are

$$P_{11}^* \vec{X}_{31} = \vec{R}_{31}^*, \quad (49)$$

in which

$$\vec{R}_{31}^* = \vec{R}_{31} + \begin{pmatrix} 0 \\ 0 \\ V_N^{(0)} R^{(2)} \rho_{11} / (R_{cr}^*)^2 - V_N^{(20)} \rho_{11} / R_{cr}^* \end{pmatrix}. \quad (50)$$

Finally, the solvability condition for the relative bifurcation point is

$$C_{31} + \left(\frac{R_{cr}^*}{k\beta} \right) E_{31}^* + \left(\frac{1}{\beta M} \right) D_{31} = 0, \quad (51)$$

in which $E_{31}^* = E_{31} + V_N^{(0)} R^{(2)} \rho_{11} / (R_{cr}^*)^2 - V_N^{(20)} \rho_{11} / R_{cr}^*$. From now on the superscript (*) notation will be dropped and the stability criterion being considered will be explicitly stated. We have compared numerical and analytical calculations of relative stability points, and again we have observed very close agreement between the results, verifying the consistency of our calculations. Fig. (5) gives a comparison between the values of the relative and the absolute critical radii given by Eqns. (48) and (6), respectively. The relative stability critical radii are larger than the absolute critical radii at any wavenumber, for fixed values of β and R_∞ . (For further details on the condition of relative marginal stability see Coriell and Hardy[12].) Fig. (5) is representative of the difference between the relative and absolute marginal stability radii for all of the parameter values for which we have examined nonlinear stability.

We investigate the subcritical and supercritical nature of the nonlinear bifurcation by evaluating the parameter $(R_{nl} - R_{cr})/A_{nl}^2$ as a function of the conductivity ratio, the parameter R_∞ and the wavenumber of the perturbation. In Fig. (6), values of the absolute bifurcation parameter $(R_{nl} - R_{cr})/A_{nl}^2$ are plotted as a function of the wavenumber for different values of β at fixed R_∞ . The results show that this parameter is almost always negative, the exceptions being at the largest values of R_∞ and β , for wavenumbers of $k = 2$ and $k = 3$. Changing the value of R_∞ does not change appreciably the features shown in Fig. (6). In Fig. (7) we show an enlarged view of a section of Fig. (6) that shows more clearly the change in sign of $(R_{nl} - R_{cr})/A_{nl}^2$ for perturbations with wavenumbers 2 and 3. In Fig. (8) we plot the parameter $(R_{nl} - R_{cr})/A_{nl}^2$ determined using the relative stability criterion. The results

show that according to the relative stability criterion, the bifurcations are nearly always subcritical except at the wavenumber $k = 3$. The qualitative behavior of the bifurcation is very similar for all cases considered for either the relative theory or the absolute theory. As the ratio of thermal conductivities decreases, or as the value of R_∞ decreases, or as the wavenumber increases, the bifurcations become more strongly subcritical.

6 Conclusions

In summary, we have used numerical and analytical methods to calculate consistently nonlinear bifurcations for the fundamental Fourier component of the local normal growth speed of a crystal-melt interface during the free growth of a pure single crystal. The analytical results correspond to an instantaneous condition for the nonlinear stability of a given Fourier shape component, and represent the first application of weakly nonlinear stability analysis to problems in solidification theory for which the unperturbed state is not steady. Our numerical method is based on a boundary integral technique. The analytical analysis provides an important check on the numerical method, which can then be used with confidence to compute finite amplitude solutions. Using the numerical solution technique, we have shown that at a fixed radius, the fundamental component, $V_N(k, A)$, of the local normal growth speed obeys a Landau-type equation. Furthermore, the higher order components of the velocity are proportional to powers in A , for small amplitude perturbations. We find that the fundamental Fourier component of the local normal growth speed vanishes at a critical amplitude, in agreement with results obtained from an expansion technique to calculate an-

alytically this critical amplitude. Two stability criteria are considered; these correspond to the relative and the absolute stability criteria. For the absolute criterion, our results show that the nonlinear bifurcations are almost always subcritical, except at high conductivity ratios and high values of R_∞ for wavenumbers $k = 2$ and $k = 3$. For the relative stability criterion, the bifurcations are nearly always subcritical except for high values of R_∞ and wavenumber $k = 3$. Furthermore, as the ratio of the solid to liquid thermal conductivity increases and the outer boundary radius increases, the bifurcations become less strongly subcritical. We also show that for fixed thermal conductivity ratio and R_∞ , the bifurcation becomes more strongly subcritical as the wavenumber increases. Although our results are only strictly applicable to the specific model that we have treated, several broader inferences can be made. First, the fact that the results from numerical computations and from weakly nonlinear stability analyses are in such good agreement is not only comforting but suggests that weakly nonlinear analyses, in general, make sense and capture the most important nonlinearities near the onset of instability. This has been appreciated previously for steady state base states, but our analysis extends this influence to non steady state base states as well. Second, almost all of the bifurcations that we have examined are subcritical and, although we cannot yet explain why, one is led to suppose that this is due to some underlying physical mechanism that we should seek to uncover. One wonders, moreover, if the same results (subcritical bifurcations) would be found for a growing sphere, and this is currently being investigated. Finally, we note that the nonlinear analysis may be generalized to include the effects of linear isotropic interfacial attachment kinetics; however, it is not anticipated that

the kinetic effects will significantly alter the results presented in this analysis, other than to delay the onset of morphological instability of the crystal to higher values of R .

References

- [1] D.J. Wollkind and L.A. Segal. *Phil. Trans. Roy. Soc. London*, 268:p. 351, 1970.
- [2] J.I.D. Alexander, D.J. Wollkind, and R.F. Sekerka. *J. Cryst. Growth*, 79:p. 849, 1986.
- [3] R. Sriranganathan, D.J. Wollkind, and D.B. Oulton. *J. Cryst. Growth*, 62:p. 265, 1983.
- [4] D.J. Wollkind, R. Sriranganathan, and D. Oulton. *Physica D*, 12:p. 215, 1984.
- [5] A.A. Wheeler. *IMA J. Appl. Math.*, 35:p. 131, 1985.
- [6] G.B. McFadden, R.F. Boisvert, and S.R. Coriell. *J. Cryst. Growth*, 84:p. 371, 1987.
- [7] L.H. Ungar and R.A. Brown. *Phys. Rev. B*, 30:p. 3993, 1984.
- [8] Gregory Dee and Rajiv Mathur. *Phys. Rev. B*, 27(12):p. 7073, 1983.
- [9] G.B. McFadden, S.R. Coriell, and R.F. Sekerka. *J. Cryst. Growth*, 91:p. 180, 1988.
- [10] L. N. Brush. PhD thesis, Department of Metallurgical Engineering and Materials Science, Carnegie-Mellon University, 1988.
- [11] L. N. Brush and R. F. Sekerka. *J. Cryst. Growth*, 96:p. 419, 1989.
- [12] S.R. Coriell and S.C. Hardy. *J. Res. Natl. Bur. Stds.*, 73A:p. 65, 1969.

[13] W.W. Mullins and R.F. Sekerka. *J. Appl. Phys.*, 35(2):p. 441, 1964.

Appendix

Definitions:

$$\Phi^{(n)} = \beta U_S^{(n)} - U_L^{(n)}, \quad M = \left(1 - \left(\frac{R_{cr}}{R_\infty}\right)^{2k}\right) / \left(1 + \left(\frac{R_{cr}}{R_\infty}\right)^{2k}\right)$$

$$\text{and } M_4 = \left(1 - \left(\frac{R_{cr}}{R_\infty}\right)^{4k}\right) / \left(1 + \left(\frac{R_{cr}}{R_\infty}\right)^{4k}\right).$$

The coefficients in the expansion are:

$$C_1 = D_1 = E_1 = 0$$

$$C_2 = -\frac{(Z^{(1)})^2}{R_{cr}^3} - \frac{(Z_\theta^{(1)})^2}{2R_{cr}^3} - \frac{2Z^{(1)}Z_{\theta\theta}^{(1)}}{R_{cr}^3} - \frac{(Z^{(1)})^2}{2} \left(\frac{d^2U_S^{(0)}}{dr^2}\right)_{R_{cr}} - (Z^{(1)}) \left(\frac{\partial U_S^{(1)}}{\partial r}\right)_{R_{cr}}$$

$$D_2 = -\frac{(Z^{(1)})^2}{R_{cr}^3} - \frac{(Z_\theta^{(1)})^2}{2R_{cr}^3} - \frac{2Z^{(1)}Z_{\theta\theta}^{(1)}}{R_{cr}^3} - \frac{(Z^{(1)})^2}{2} \left(\frac{d^2U_L^{(0)}}{dr^2}\right)_{R_{cr}} - (Z^{(1)}) \left(\frac{\partial U_L^{(1)}}{\partial r}\right)_{R_{cr}}$$

$$E_2 = \frac{(Z^{(1)})^2}{2} \left(\frac{d^3\Phi^{(0)}}{dr^3}\right)_{R_{cr}} + Z^{(1)} \left(\frac{\partial^2\Phi^{(1)}}{\partial r^2}\right)_{R_{cr}} - \left(\frac{Z_\theta^{(1)}}{R_{cr}^2}\right) \left(\frac{\partial\Phi^{(1)}}{\partial\theta}\right)_{R_{cr}} \\ - \left(\frac{(Z_\theta^{(1)})^2}{2R_{cr}^2}\right) \left(\frac{d\Phi^{(0)}}{dr}\right)_{R_{cr}}$$

$$C_3 = -\left(\frac{2Z^{(1)}Z^{(2)}}{R_{cr}^3}\right) + \left(\frac{(Z^{(1)})^3}{R_{cr}^4}\right) - \left(\frac{Z_\theta^{(1)}Z_\theta^{(2)}}{R_{cr}^3}\right) + \\ \left(\frac{3(Z_\theta^{(1)})^2Z^{(1)}}{2R_{cr}^4}\right) - \left(\frac{2Z_{\theta\theta}^{(2)}Z^{(1)}}{R_{cr}^3}\right) - \left(\frac{2Z_{\theta\theta}^{(1)}Z^{(2)}}{R_{cr}^3}\right) + \\ \left(\frac{3(Z^{(1)})^2Z_{\theta\theta}^{(1)}}{R_{cr}^4}\right) - \left(\frac{3Z_{\theta\theta}^{(1)}(Z_\theta^{(1)})^2}{2R_{cr}^4}\right) \\ - Z^{(1)}Z^{(2)} \left(\frac{d^2U_S^{(0)}}{dr^2}\right)_{R_{cr}} - \frac{(Z^{(1)})^3}{6} \left(\frac{d^3U_S^{(0)}}{dr^3}\right)_{R_{cr}} - Z^{(2)} \left(\frac{\partial U_S^{(1)}}{\partial r}\right)_{R_{cr}}$$

$$\begin{aligned}
& -\frac{(Z^{(1)})^2}{2} \left(\frac{\partial^2 U_S^{(1)}}{\partial r^2} \right)_{R_{cr}} - Z^{(1)} \left(\frac{\partial U_S^{(2)}}{\partial r} \right)_{R_{cr}} \\
D_3 = & -\left(\frac{2Z^{(1)}Z^{(2)}}{R_{cr}^3} \right) + \left(\frac{(Z^{(1)})^3}{R_{cr}^4} \right) - \left(\frac{Z_\theta^{(1)}Z_\theta^{(2)}}{R_{cr}^3} \right) + \\
& \left(\frac{3(Z_\theta^{(1)})^2Z^{(1)}}{2R_{cr}^4} \right) - \left(\frac{2Z_{\theta\theta}^{(2)}Z^{(1)}}{R_{cr}^3} \right) - \left(\frac{2Z_{\theta\theta}^{(1)}Z^{(2)}}{R_{cr}^3} \right) + \\
& \left(\frac{3(Z^{(1)})^2Z_{\theta\theta}^{(1)}}{R_{cr}^4} \right) - \left(\frac{3Z_{\theta\theta}^{(1)}(Z_\theta^{(1)})^2}{2R_{cr}^4} \right) \\
& -Z^{(1)}Z^{(2)} \left(\frac{d^2 U_L^{(0)}}{dr^2} \right)_{R_{cr}} - \frac{(Z^{(1)})^3}{6} \left(\frac{d^3 U_L^{(0)}}{dr^3} \right)_{R_{cr}} - Z^{(2)} \left(\frac{\partial U_L^{(1)}}{\partial r} \right)_{R_{cr}} \\
& -\frac{(Z^{(1)})^2}{2} \left(\frac{\partial^2 U_L^{(1)}}{\partial r^2} \right)_{R_{cr}} - Z^{(1)} \left(\frac{\partial U_L^{(2)}}{\partial r} \right)_{R_{cr}} \\
E_3 = & Z^{(1)}Z^{(2)} \left(\frac{d^3 \Phi^{(0)}}{dr^3} \right)_{R_{cr}} + \frac{(Z^{(1)})^3}{6} \left(\frac{d^4 \Phi^{(0)}}{dr^4} \right)_{R_{cr}} + Z^{(2)} \left(\frac{\partial^2 \Phi^{(1)}}{\partial r^2} \right)_{R_{cr}} \\
& + \frac{(Z^{(1)})^2}{2} \left(\frac{\partial^3 \Phi^{(1)}}{\partial r^3} \right)_{R_{cr}} + Z^{(1)} \left(\frac{\partial^2 \Phi^{(2)}}{\partial r^2} \right)_{R_{cr}} \\
& - \left(\frac{Z^{(1)}Z_\theta^{(1)}}{R_{cr}^2} \right) \left(\frac{\partial^2 \Phi^{(1)}}{\partial r \partial \theta} \right)_{R_{cr}} - \left(\frac{Z_\theta^{(2)}}{R_{cr}^2} \right) \left(\frac{\partial \Phi^{(1)}}{\partial \theta} \right)_{R_{cr}} \\
& + \left(\frac{2Z^{(1)}Z_\theta^{(1)}}{R_{cr}^3} \right) \left(\frac{\partial \Phi^{(1)}}{\partial \theta} \right)_{R_{cr}} - \left(\frac{Z_\theta^{(1)}}{R_{cr}^2} \right) \left(\frac{\partial \Phi^{(2)}}{\partial \theta} \right)_{R_{cr}} \\
& - \left(\frac{(Z_\theta^{(1)})^2}{2R_{cr}^2} \right) \left(\frac{\partial \Phi^{(1)}}{\partial r} \right)_{R_{cr}} - \left(\frac{Z^{(1)}(Z_\theta^{(1)})^2}{2R_{cr}^2} \right) \left(\frac{d^2 \Phi^{(0)}}{dr^2} \right)_{R_{cr}} + \left(\frac{Z^{(1)}(Z_\theta^{(1)})^2}{R_{cr}^3} \right) \left(\frac{d\Phi^{(0)}}{dr} \right)_{R_{cr}}
\end{aligned}$$

$$C_{20} = [2k^3 + 3k^2 - 2k - 2] \frac{\rho_{11}^2}{4R_{cr}^3}$$

$$C_{22} = [2k^3 + 5k^2 - 2k - 2] \frac{\rho_{11}^2}{4R_{cr}^3}$$

$$D_{20} = \left(\frac{1}{4R_{cr}^3 M} [2k - 2k^3 + 3k^2 M - 2M] + \frac{B_L^{(0)}}{4R_{cr}^2 M} [M - 2k] \right) \rho_{11}^2$$

$$D_{22} = \left(\frac{1}{4R_{cr}^3 M} [2k - 2k^3 + 5k^2 M - 2M] + \frac{B_L^{(0)}}{4R_{cr}^2 M} [M - 2k] \right) \rho_{11}^2$$

$$E_{20} = \left[\frac{B_L^{(0)}((Mk^2/2) + k - M)}{2MR_{cr}^3} - \frac{k(1-k^2)(1+\beta M)}{2MR_{cr}^4} \right] \rho_{11}^2$$

$$E_{22} = \left[\frac{B_L^{(0)}}{2MR_{cr}^3} \left((3Mk^2/2) + k - M \right) - \frac{k(1-k^2)}{2MR_{cr}^4} (2kM + 1 - (2k-1)M\beta) \right] \rho_{11}^2$$

$$C_{31} = -R^{(2)} \left[\frac{-1}{R_{cr}^3} (k^3 + 2k^2 - k - 2) \right] \rho_{11} + \left[\frac{1}{4R_{cr}^4} (k^4 - (13/2)k^3 - 7k^2 + (7/2)k + 3) \right] \rho_{11}^3$$

$$D_{31} = -R^{(2)} \left[\frac{1}{R_{cr}^3} \left(\frac{k^3}{M} - 2k^2 - \frac{k}{M} + 2 + \frac{1}{\ln(R_{cr}/R_\infty)} \right) \right] \rho_{11}$$

$$-R^{(2)} \left[\frac{B_L^{(0)}}{R_{cr}^2} \left(\frac{k}{M} - \left(1 + \frac{1}{\ln(R_{cr}/R_\infty)} \right) \right) \right] \rho_{11}$$

$$\left[\frac{1}{4R_{cr}^4} \left(k^4 \left(3 - \frac{2}{MM_4} \right) + k^3 \left(\frac{3}{2M} + \frac{2}{M \ln(R_{cr}/R_\infty)} + \frac{5}{M_4} \right) \right) \right] \rho_{11}^3 +$$

$$\left[\frac{1}{4R_{cr}^4} \left(k^2 \left(-9 - \frac{3}{\ln(R_{cr}/R_\infty)} + \frac{2}{MM_4} \right) \right) \right] \rho_{11}^3 +$$

$$\left[\frac{1}{4R_{cr}^4} \left(k \left(-\frac{3}{2M} - \frac{2}{M_4} - \frac{2}{M \ln(R_{cr}/R_\infty)} \right) + 3 + \frac{2}{\ln(R_{cr}/R_\infty)} \right) \right] \rho_{11}^3 +$$

$$\left[\frac{B_L^{(0)}}{4R_{cr}^3} \left(k^2 \left(\frac{3}{2} - \frac{2}{MM_4} \right) + k \left(\frac{1}{M_4} + \frac{3}{2M} + \frac{2}{M \ln(R_{cr}/R_\infty)} \right) \right) \right] \rho_{11}^3 -$$

$$\left[\frac{B_L^{(0)}}{4R_{cr}^3} \left(1 + \frac{1}{\ln(R_{cr}/R_\infty)} \right) \right] \rho_{11}^3$$

$$E_{31} = -R^{(2)} \left[\frac{B_L^{(0)}}{R_{cr}^3} \left(-k^2 - k/M + 2 + \frac{1}{\ln(R_{cr}/R_\infty)} \right) \right] \rho_{11} +$$

$$\begin{aligned}
& -R^{(2)} \left[\frac{1}{R_{cr}^4} \left(k^4(\beta - 1) - k^3(\beta + 1/M) + k^2(1 - \beta) \right) \right] \rho_{11} + \\
& -R^{(2)} \left[\frac{1}{R_{cr}^4} \left(k(\beta + 1/M) - \frac{1}{\ln(R_{cr}/R_\infty)} \right) \right] \rho_{11} \\
& + \left[\frac{B_L^{(0)}}{R_{cr}^4} \left(k^3 \left(\frac{3}{8M} \right) + k^2 \left(\frac{4}{8MM_4} - \frac{9}{8} \right) \right) \right] \rho_{11}^3 + \\
& \left[\frac{B_L^{(0)}}{R_{cr}^4} \left(k \left(-\frac{6}{8M} - \frac{2}{8M_4} - \frac{4}{8M \ln(R_{cr}/R_\infty)} \right) + \left(\frac{3}{4} + \frac{1}{4 \ln(R_{cr}/R_\infty)} \right) \right) \right] \rho_{11}^3 + \\
& \left[\frac{1}{R_{cr}^5} \left(k^5 \left(\frac{3(\beta + 1/M)}{8} \right) + k^4 \left(\frac{11\beta}{8} + \frac{4}{8MM_4} - \frac{15}{8} \right) \right) \right] \rho_{11}^3 + \\
& \left[\frac{1}{R_{cr}^5} \left(k^3 \left(-\frac{9}{8M} - \frac{19\beta}{8} - \frac{10}{8M_4} - \frac{4}{8M \ln(R_{cr}/R_\infty)} \right) \right) \right] \rho_{11}^3 + \\
& \left[\frac{1}{R_{cr}^5} \left(k^2 \left(\frac{9}{8} - \frac{5\beta}{8} + \frac{6}{8 \ln(R_{cr}/R_\infty)} - \frac{4}{8MM_4} \right) \right) \right] \rho_{11}^3 + \\
& \left[\frac{1}{R_{cr}^5} \left(k \left(\frac{10\beta}{8} + \frac{6}{8M} + \frac{4}{8M_4} + \frac{4}{8M \ln(R_{cr}/R_\infty)} \right) - \left(\frac{4}{8 \ln(R_{cr}/R_\infty)} \right) \right) \right] \rho_{11}^3 \\
-\Upsilon = & \left[\frac{1}{\beta R_{cr}^3} \left(1 - \frac{1}{M^2} \right) \right] k^3 + \left[\frac{3}{R_{cr}^3} \left(1 + \frac{1}{\beta M} \right) \right] k^2 + \\
& \left[\frac{1}{\beta R_{cr}^2} \left(1 - \frac{1}{M^2} \right) \left(B_L^{(0)} - \frac{1}{R_{cr}} \right) \right] k + \\
& \left[-\frac{3}{R_{cr}^3} \left(1 + \frac{1}{\beta M} \right) + \left(\frac{2B_L^{(0)}}{M\beta R_{cr}^2} \right) + \left(B_L^{(0)} - \frac{1}{R_{cr}} \right) \left(\frac{1}{M\beta R_{cr}^2 \ln(R_{cr}/R_\infty)} \right) \right] + \\
& \left[-\left(\frac{2B_L^{(0)}}{\beta R_{cr}^2} \right) - \left(\frac{1}{\beta R_{cr}^2 \ln(R_{cr}/R_\infty)} \right) \left(B_L^{(0)} - \frac{1}{R_{cr}} \right) \right] \frac{1}{k} \\
\Omega = & \left[\frac{5}{8R_{cr}^4} + \frac{9}{8M\beta R_{cr}^4} - \frac{4}{8M^2 M_4 \beta R_{cr}^4} \right] k^4 + \\
& \left[\frac{-2}{8R_{cr}^4} - \frac{15}{8\beta R_{cr}^4} + \frac{14}{8MM_4\beta R_{cr}^4} + \frac{3}{8M^2\beta R_{cr}^4} + \frac{4}{8M^2\beta R_{cr}^4 \ln(R_{cr}/R_\infty)} \right] k^3 +
\end{aligned}$$

$$\begin{aligned}
& \left[-\frac{33}{8R_{cr}^4} - \frac{27}{8M\beta R_{cr}^4} - \frac{10}{8M_4\beta R_{cr}^4} - \frac{10}{8M\beta R_{cr}^4 \ln(R_{cr}/R_\infty)} \right] k^2 - \\
& \left[\frac{4}{8M^2 M_4 \beta R_{cr}^3} \left(B_L^{(0)} - \frac{1}{R_{cr}} \right) - \frac{6B_L^{(0)}}{8M\beta R_{cr}^3} \right] k^2 + \\
& \left[\frac{2}{8R_{cr}^4} + \frac{9}{8\beta R_{cr}^4} - \frac{9B_L^{(0)}}{8\beta R_{cr}^3} + \frac{6B_L^{(0)}}{8MM_4\beta R_{cr}^3} - \frac{1}{MM_4\beta R_{cr}^4} \right] k + \\
& \left[\frac{3}{8M^2\beta R_{cr}^3} \left(B_L^{(0)} - \frac{1}{R_{cr}} \right) + \frac{6}{8\beta R_{cr}^4 \ln(R_{cr}/R_\infty)} + \frac{4}{8M^2\beta R_{cr}^3 \ln(R_{cr}/R_\infty)} \left(B_L^{(0)} - \frac{1}{R_{cr}} \right) \right] k + \\
& \left[\frac{16}{8R_{cr}^4} + \frac{12}{8M\beta R_{cr}^4} - \frac{8B_L^{(0)}}{8M\beta R_{cr}^3} - \frac{2B_L^{(0)}}{8M_4\beta R_{cr}^3} + \frac{8}{8M\beta R_{cr}^4 \ln(R_{cr}/R_\infty)} \right] - \\
& \left[\frac{6B_L^{(0)}}{8M\beta R_{cr}^3 \ln(R_{cr}/R_\infty)} - \frac{4}{8M_4\beta R_{cr}^4} \right] + \\
& \left[\frac{6B_L^{(0)}}{8\beta R_{cr}^3} + \frac{2B_L^{(0)}}{8\beta R_{cr}^3 \ln(R_{cr}/R_\infty)} - \frac{4}{8\beta R_{cr}^4 \ln(R_{cr}/R_\infty)} \right] \frac{1}{k}
\end{aligned}$$

Table 1: $V_N(nk, A)$ as a function of A . The numerical results show that in the regime $A \ll 1$, $V_N(nk, A) = C_n A^n$. The example shown in this table is for the case given by the curve labelled as (3) in Fig. (1).

Fundamental Component

n	C_n
1	$C_1 = -.452 \times 10^{-8}$
2	$C_2 = +.363 \times 10^{-7}$
3	$C_3 = -.853 \times 10^{-9}$

Table 2: Numerically and analytically determined values of A_{nl} for $\beta = 1$, $R_\infty = 10^6$, $R_{cr} = 322.56787$ and $k = 4$.

Critical Amplitude

R	A_{nl} (num)	A_{nl} (ana)
322.564	.730 to .731	.730504
322.563	.819 to .820	.819279
322.562	.899 to .900	.899333

Table 3: Analytically calculated values of $A_{nl}/(R_{cr} - R_{nl})^{1/2}$ as a function of R_∞ , using the absolute stability criterion for $\beta = 1$.

Analytical Analysis

R_∞	$A_{nl}/(R_{cr} - R_{nl})^{1/2}$
10^5	14.40900
10^6	16.66126
5×10^6	18.10505
10^7	18.69906
5×10^7	20.02192

Table 4: Analytically calculated values of $A_{nl}/(R_{cr} - R_{nl})^{1/2}$ as a function of β , using the absolute stability criterion for $R_\infty = 10^6$.

Analytical Analysis

β	$A_{nl}/(R_{cr} - R_{nl})^{1/2}$
.5	13.16962
1.0	16.66126
2.0	22.81829

Figure Captions

Figure 1. The fundamental Fourier component of the velocity $V_N(k, A)$ as a function of A .

Here $\beta = 1$, the value of R_∞ is 10^6 , $R_{cr} = 322.5678$ and $k = 4$. Curves (1), (2) and (3) are for radii $R = 322.55$, 322.4 and 322.2 , respectively.

Figure 2. The fundamental Fourier component of the velocity $V_N(k, A)$ as a function of A .

Here $\beta = 2$, the value of R_∞ is 10^6 , $R_{cr} = 461.8201$ and $k = 4$. Curves (1), (2) and (3) are for radii $R = 461.6$, 461.5 and 461.4 , respectively.

Figure 3. A_{nl} as a function of R plotted for the conditions given in Fig. (1).

Figure 4. A plot of $\ln(A_{nl})$ vs. $1/2 \ln(R_{cr} - R_{nl})$. The solid line is the analytical solution given by the weakly nonlinear analysis and the open boxes are the values from the numerical calculations. In this case, $\beta = 1$ and $R_\infty = 10^6$. The slope is unity.

Figure 5. A comparison between the values of the critical radii using the absolute stability criterion and the relative stability criterion. The anomalous case $k = 2$ for the relative stability criterion is omitted because, formally, the critical radius becomes very large.

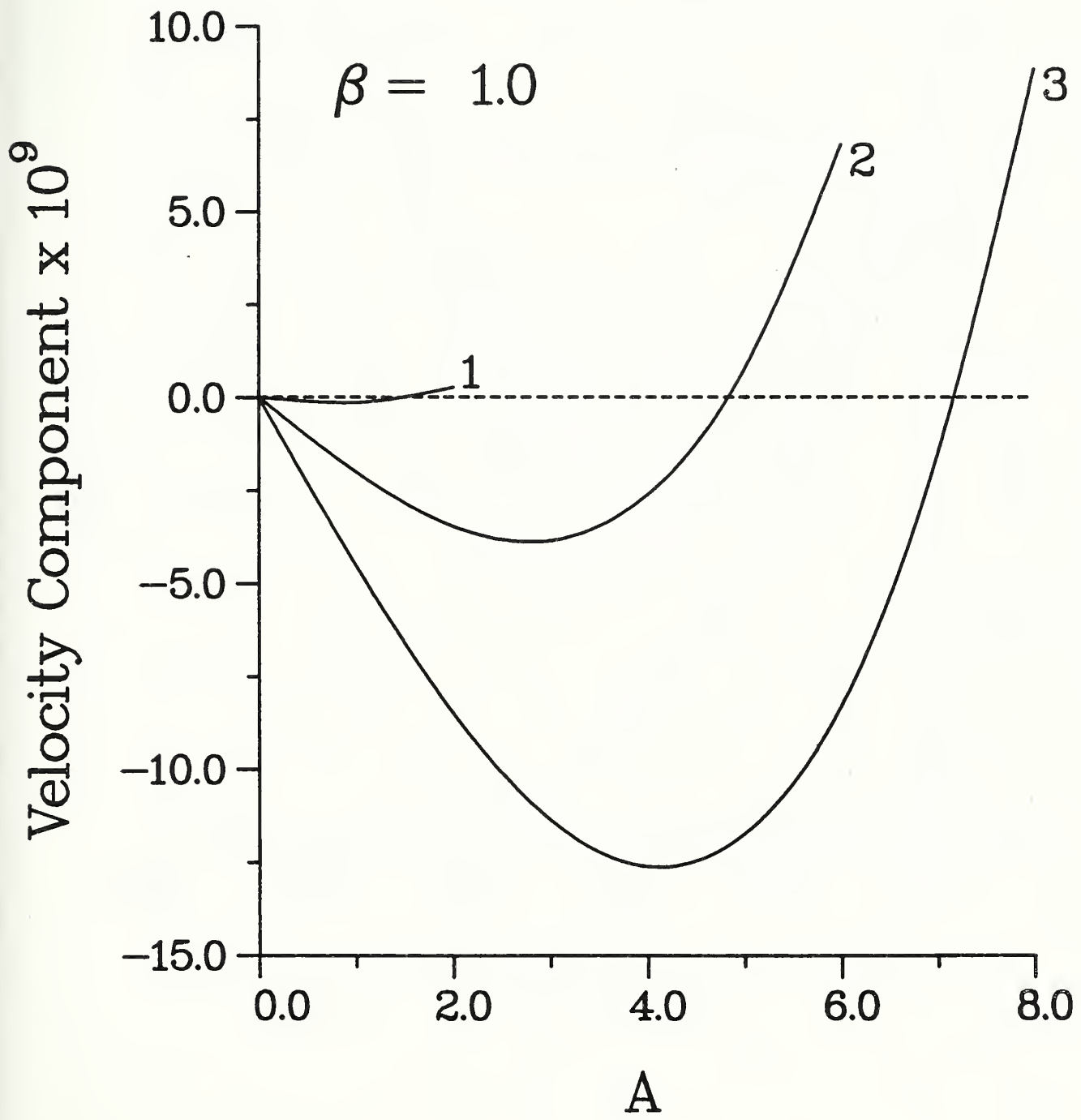
Figure 6. A plot of $(R_{nl} - R_{cr})/A_{nl}^2$ using the absolute stability criterion. The curves are for values of β equal to $1/2$, 1 , 2 and 4 . The value of $R_\infty = 10^8$.

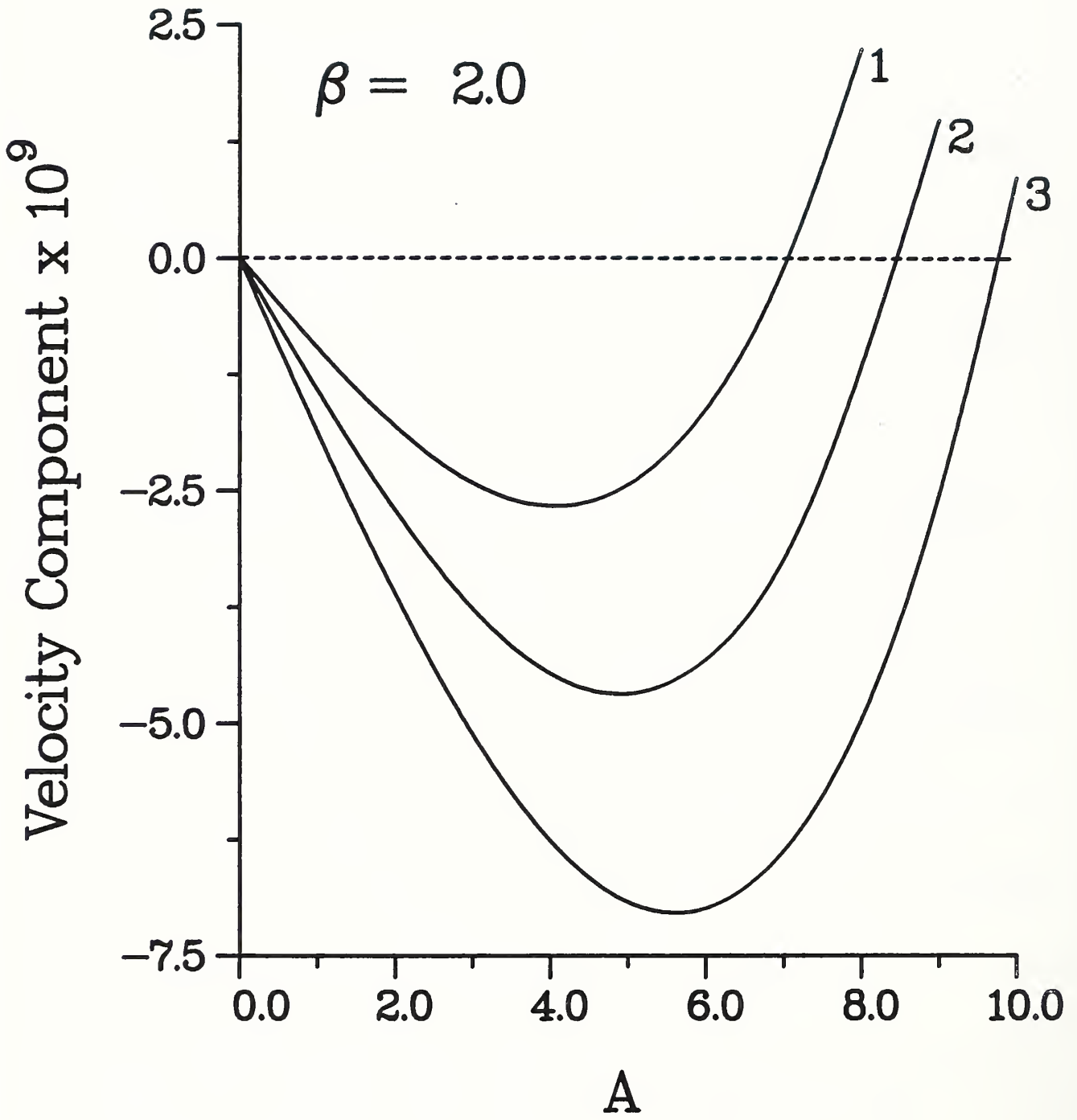
Figure 7. A plot of $(R_{nl} - R_{cr})/A_{nl}^2$ using the absolute stability criterion. The curves are for values of β equal to 1 , 2 and 4 . The plots are taken from a section of the plot in Fig. (6) and reveal the positive values of the parameter $(R_{nl} - R_{cr})/A_{nl}^2$ for perturbations

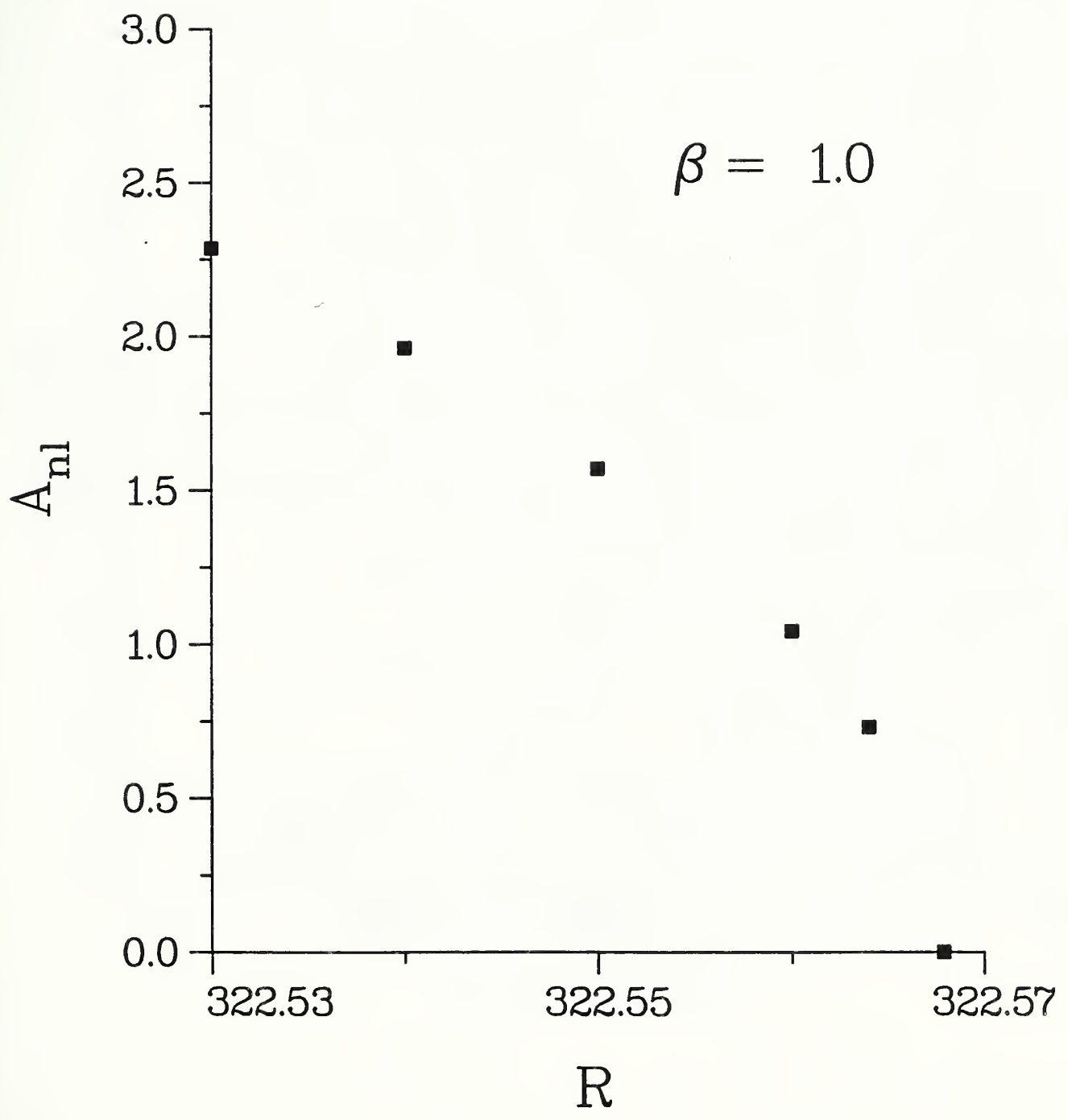
of wavenumber $k = 2$ and $k = 3$.

Figure 8. A plot of $(R_{nl} - R_{cr})/A_{nl}^2$ using the relative stability criterion. The curves correspond to values of β equal to $1/2$, 1 , 2 and 4 . The value of $R_{\infty} = 10^8$.

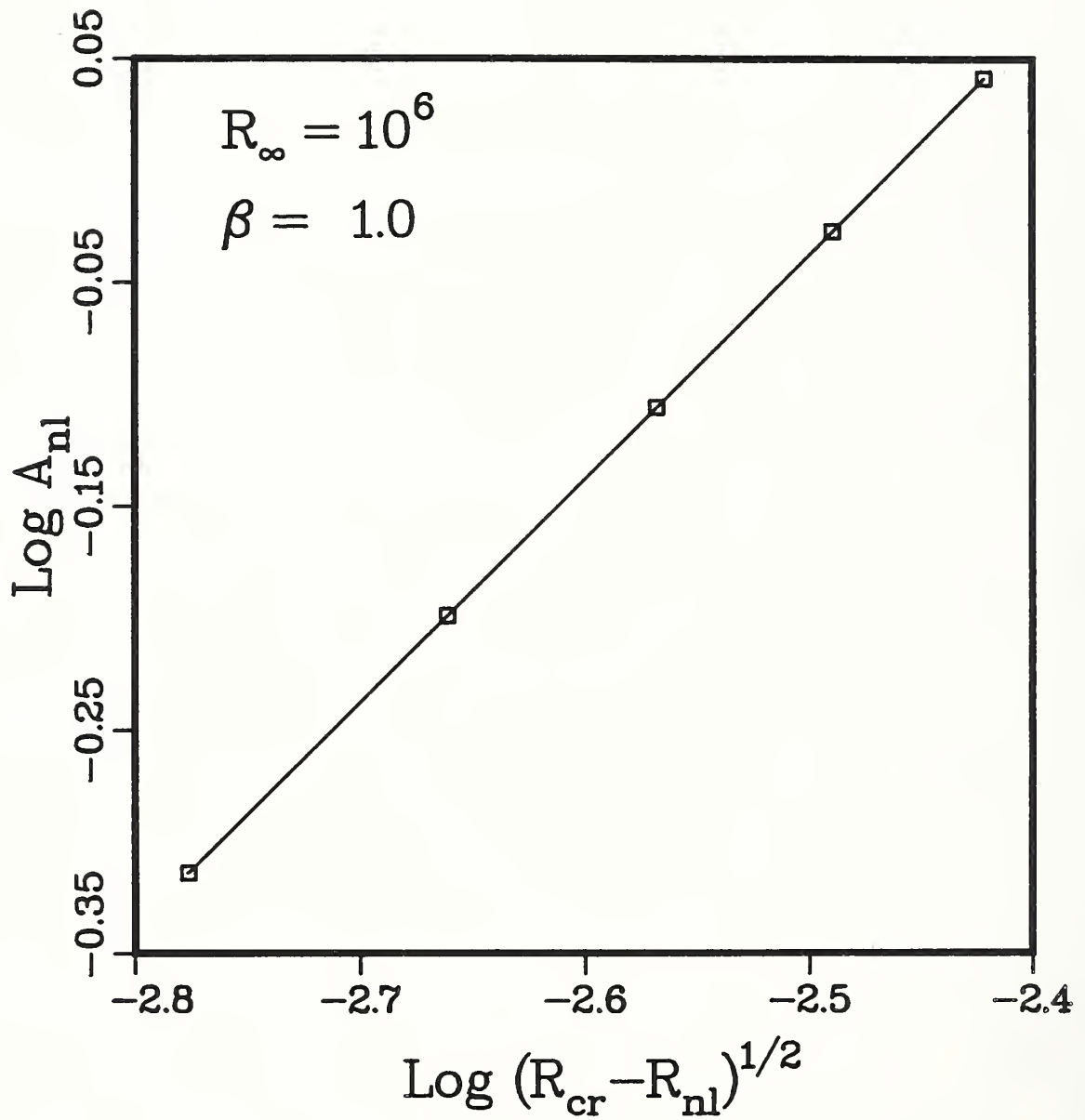
FIG. 1



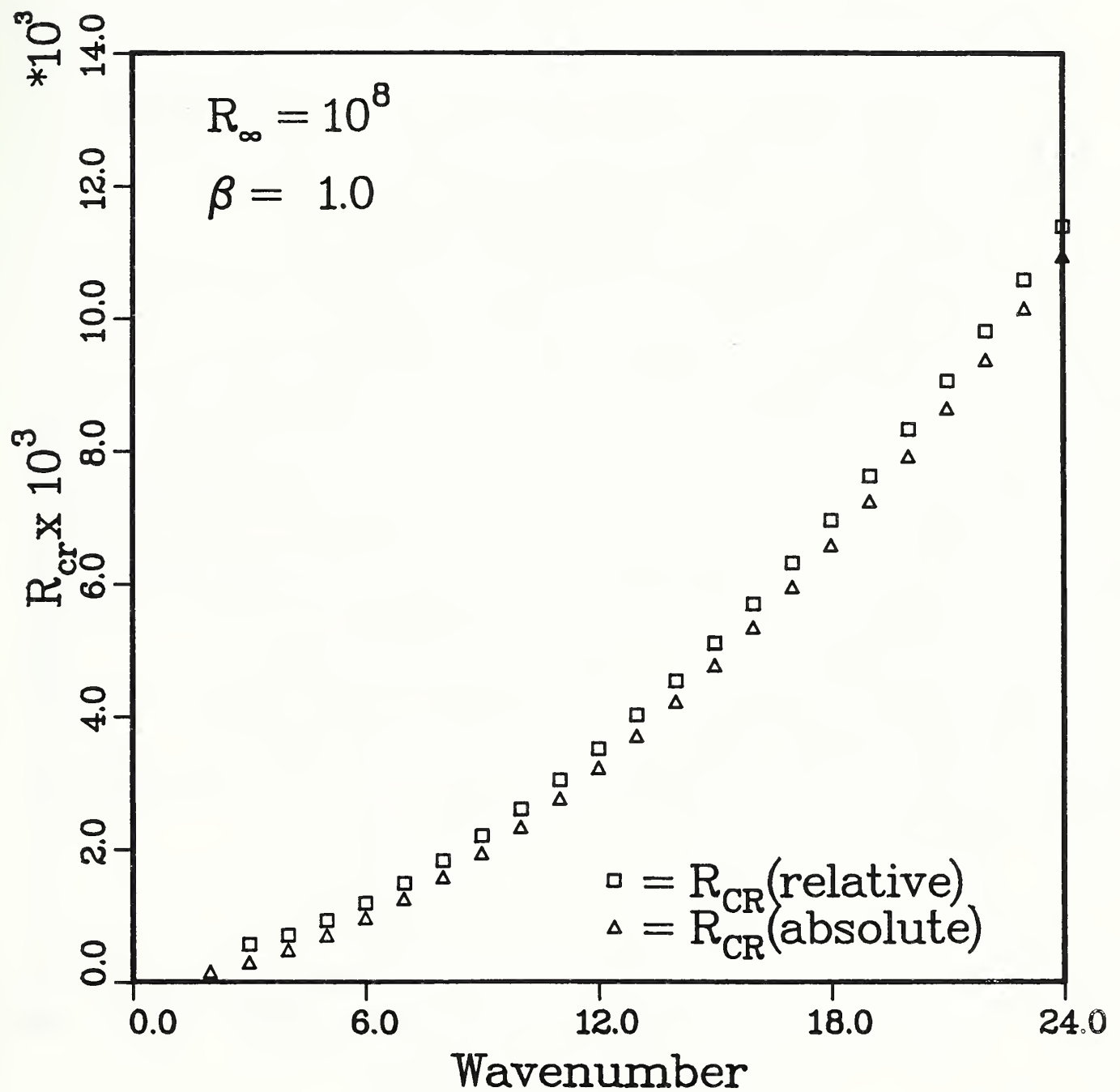




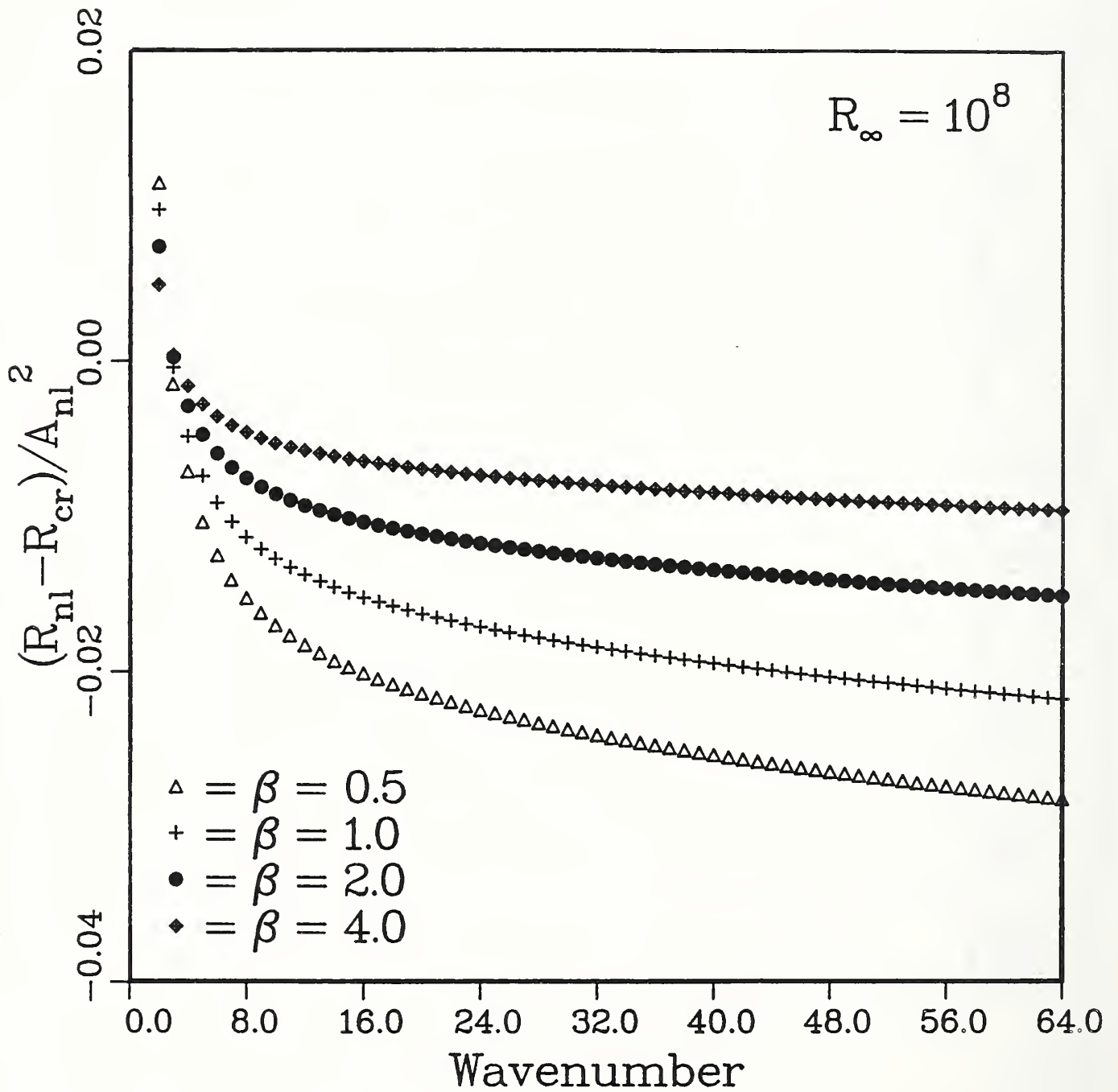
Critical Amplitude



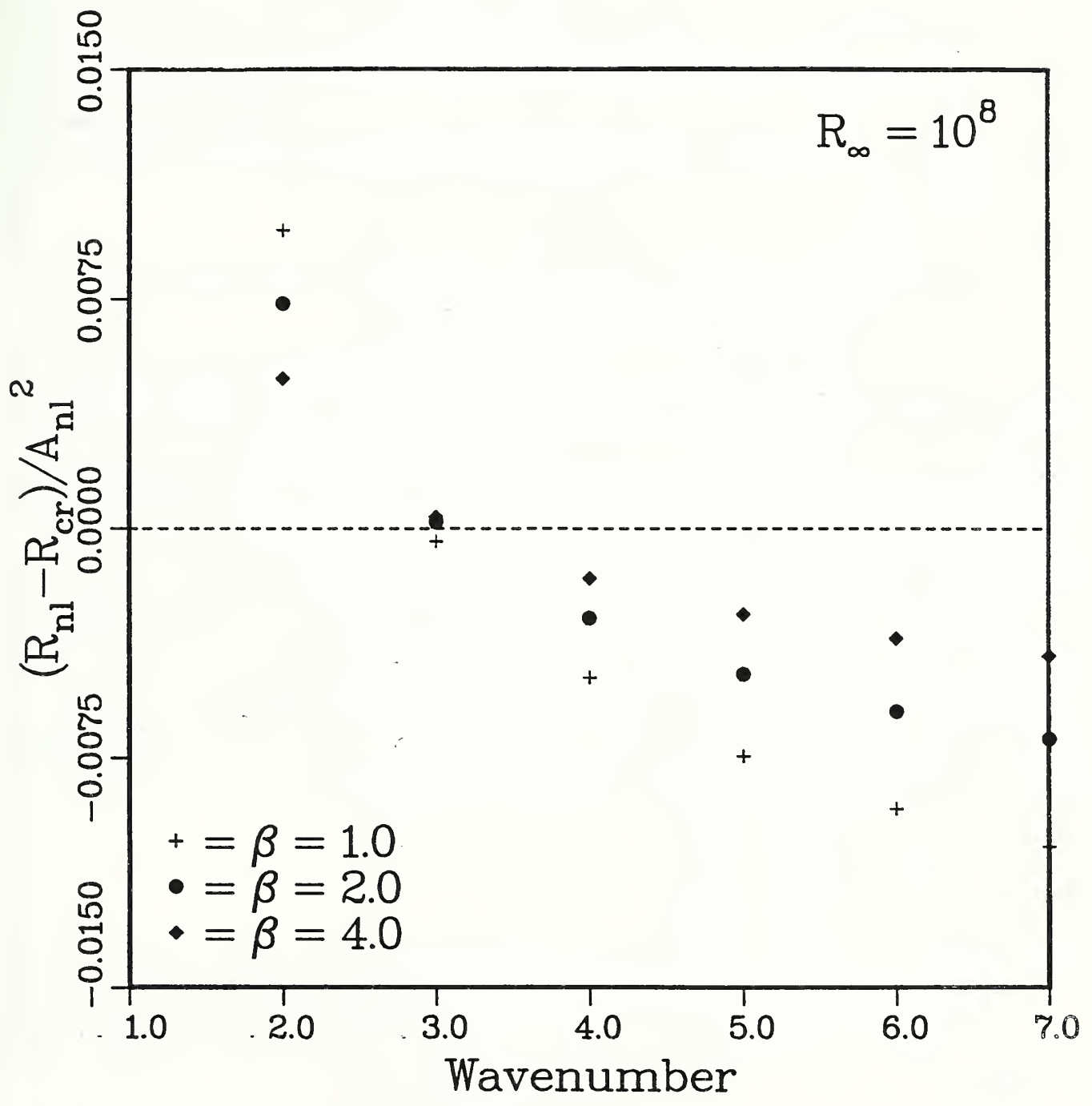
Critical Radii



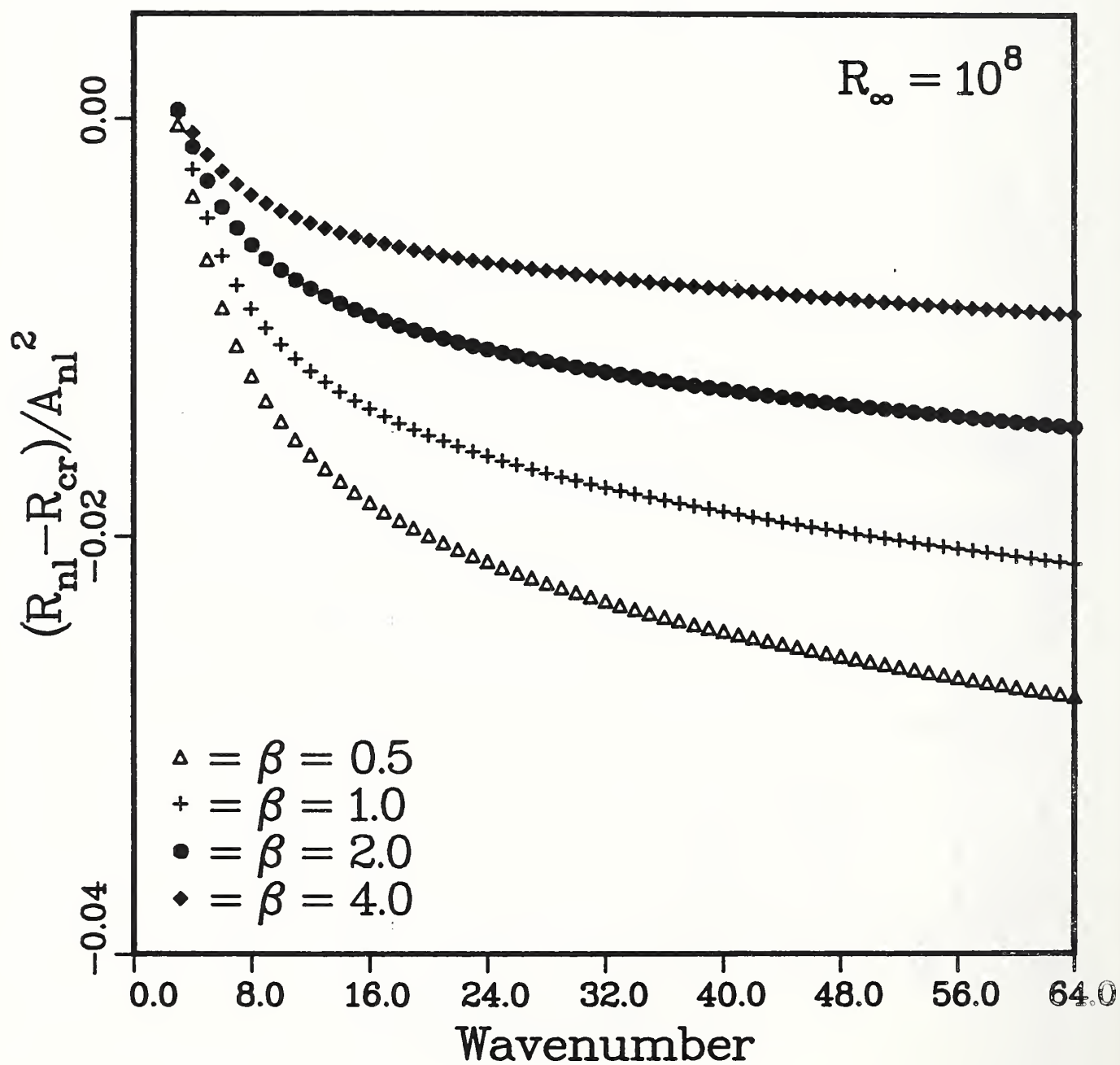
Absolute Stability



Absolute Stability



Relative Stability



U.S. DEPT. OF COMM. BIBLIOGRAPHIC DATA SHEET (See instructions)	1. PUBLICATION OR REPORT NO. NISTIR 89-4193	2. Performing Organ. Report No.	3. Publication Date OCTOBER 1989
4. TITLE AND SUBTITLE <p>A Numerical and Analytical Study of Nonlinear Bifurcations Associated with the Morphological Stability of Two-Dimensional Single Crystals</p>			
5. AUTHOR(S) L.N. Brush, R.F. Sekerka and G.B. McFadden			
6. PERFORMING ORGANIZATION (If joint or other than NBS, see instructions) NATIONAL BUREAU OF STANDARDS DEPARTMENT OF COMMERCE WASHINGTON, D.C. 20234		7. Contract/Grant No.	8. Type of Report & Period Covered
9. SPONSORING ORGANIZATION NAME AND COMPLETE ADDRESS (Street, City, State, ZIP)			
10. SUPPLEMENTARY NOTES <input type="checkbox"/> Document describes a computer program; SF-185, FIPS Software Summary, is attached.			
11. ABSTRACT (A 200-word or less factual summary of most significant information. If document includes a significant bibliography or literature survey, mention it here) <p>The nonlinear stability of a two-dimensional single crystal of pure material in an under-cooled melt is studied both analytically and numerically. The quasi-steady state approximation is used for the thermal fields and the effects of different solid and liquid thermal conductivities, isotropic interfacial growth kinetics and isotropic surface tension are included. The bifurcation analysis is performed by calculating the instantaneous value of the fundamental component of the local normal growth speed for an interface perturbed by a single Fourier shape component. Numerically, the fundamental component of the interfacial growth speed is found by Fourier analysis of the solution to an integro-differential equation obeyed at the interface. Analytically, an expansion technique is used to derive a solvability condition defining each of these bifurcation points. Our analytical and numerical results are in very close agreement. Almost all of the bifurcations are subcritical and we present our results by giving values of the Landau coefficient as a function of the different dimensionless parameters used in the model.</p>			
12. KEY WORDS (Six to twelve entries; alphabetical order; capitalize only proper names; and separate key words by semicolons) bifurcation; boundary integral; crystal growth; numerical solution; relative stability; subcritical; weakly nonlinear analysis			
13. AVAILABILITY <input checked="" type="checkbox"/> Unlimited <input type="checkbox"/> For Official Distribution. Do Not Release to NTIS <input type="checkbox"/> Order From Superintendent of Documents, U.S. Government Printing Office, Washington, D.C. 20402. <input checked="" type="checkbox"/> Order From National Technical Information Service (NTIS), Springfield, VA. 22161		14. NO. OF PRINTED PAGES 42	15. Price A03



